

Review Learning: Alleviating Catastrophic Forgetting with Generative Replay without Generator

Jaesung Yoo, Sunghyuk Choi, Ye Seul Yang, Suhyeon Kim, Jieun Choi, Dongkyeong Lim, Yaeji Lim, Hyung Joon Joo, Dae Jung Kim, Rae Woong Park, Hyeong-Jin Yoon, and Kwangsoo Kim

Abstract— When a deep learning model is sequentially trained on different datasets, it forgets the knowledge acquired from previous data, a phenomenon known as catastrophic forgetting. It deteriorates performance of the deep learning model on diverse datasets, which is critical in privacy-preserving deep learning (PPDL) applications based on transfer learning (TL). To overcome this, we propose “review learning” (RL), a generative-replay-based continual learning technique that does not require a separate generator. Data samples are generated from the memory stored within the synaptic weights of the deep learning model which are used to review knowledge acquired from previous datasets. The performance of RL was validated through PPDL experiments. Simulations and real-world medical multi-institutional experiments were conducted using three types of binary classification electronic health record data. In the real-world experiments, the global area under the receiver operating curve was 0.710 for RL and 0.655 for TL. Thus, RL was highly effective in retaining previously learned knowledge.

Index Terms— Continual learning, generative replay, feature visualization, knowledge distillation, privacy-preserving deep learning, electronic health record.

I. INTRODUCTION

Deep learning [1] has been achieving outstanding performance in various domains under the conditions of abundant, high-quality data [2-5]. However, such data are often not available owing to their natural scarcity [6] or data privacy issues [7, 8]. In medical machine learning applications [9, 10] and privacy-preserving deep learning (PPDL) [11, 12], transfer

learning (TL) [13, 14] is used when data are insufficient, which leverages acute knowledge learned from high-quality data. Despite its popular use [15-20], TL has a major drawback: the catastrophic forgetting problem [21, 22]. Unlike the biological brain [23-26], the deep learning model forgets knowledge derived from previous data when the model is sequentially trained on different types of data. Catastrophic forgetting is a major challenge, particularly in PPDL applications, in which the objective is to train a model to acquire knowledge from distributed privacy-sensitive data without sharing them [17].

To address this issue, there have been studies on continual learning for deep learning [27, 28]. The deep learning model may be continually trained by presenting previous and current data simultaneously, by storing previous data into a memory component and replaying them during training. Although this direct replay method exhibits promising performance [29], saving previous data for future training is not scalable when training data are accumulated [27, 30], and saving data in PPDL applications is often restricted owing to data privacy issues. As an alternative, a generative model is built to allow the main deep learning model to access a simile of the previously trained data, as the main model is transferred to another dataset [31]. This continual learning method, known as generative replay, has an improved continual learning performance compared to the standard TL [32, 33].

Generative replay is an effective continual learning method that prevents catastrophic forgetting but demands additional

This research was supported by the MHW (Ministry of Health and Welfare) of Korea after the project named DisTIL (Development of Privacy-Reinforcing Distributed Transfer-Iterative Learning Algorithm; Grant number: H119C0842), supervised by the KHIDI (Korea Health Industry Development Institute). This work was also supported by the Bio Industrial Strategic Technology Development Program (20003883) funded By the Ministry of Trade, Industry & Energy (MOTIE, Korea).

Corresponding author: Kwangsoo Kim (e-mail: kim.snuh@gmail.com)

Jaesung Yoo is with the School of Electrical Engineering, Korea University, Seoul, 02841 South Korea (e-mail: jsyoo61@korea.ac.kr).

Sunghyuk Choi and Hyeong-Jin Yoon are with the Department of Biomedical Engineering, Seoul National University College of Medicine, Seoul, 03080 South Korea (e-mail: sakebite@snu.ac.kr; hjyoon@snu.ac.kr).

Ye Seul Yang is with the Division of Endocrinology and Metabolism, Department of Internal Medicine, Uijeongbu St. Mary's Hospital, Gyeonggi-do, 11765 South Korea (e-mail: ysyang.endo@gmail.com).

Suhyeon Kim, Jieun Choi, Dongkyeong Lim, and Yaeji Lim are with the Department of Applied Statistics, Chung-Ang University, Seoul, 06794 South Korea (e-mail: suhy0118@gmail.com; chzieun@naver.com; ssodong93@naver.com; yaeji.lim@gmail.com).

Hyung Joon Joo is with the Department of Cardiology, Cardiovascular Center, College of Medicine, Korea University, Seoul, 02841 South Korea (e-mail: drjoohj@gmail.com).

Dae Jung Kim is with the Department of Endocrinology and Metabolism, School of Medicine, Ajou University, Gyeonggi-do, 16499 South Korea (e-mail: djkim@ajou.ac.kr).

Rae Woong Park is with the Department of Biomedical Informatics, School of Medicine, Ajou University, Gyeonggi-do, 16499 South Korea (e-mail: veritas@ajou.ac.kr).

Kwangsoo Kim is with the Transdisciplinary Department of Medicine & Advanced Technology, Seoul National University Hospital, Seoul, 03080 South Korea (e-mail: kim.snuh@gmail.com).

This article has supplementary downloadable material available at <http://ieeexplore.ieee.org>, provided by the authors.

Color versions of one or more of the figures in this article are available online at <http://ieeexplore.ieee.org>.

This work has been submitted to the IEEE for possible publication. Copyright may be transferred without notice, after which this version may no longer be accessible.

> REPLACE THIS LINE WITH YOUR MANUSCRIPT ID NUMBER (DOUBLE-CLICK HERE TO EDIT) <

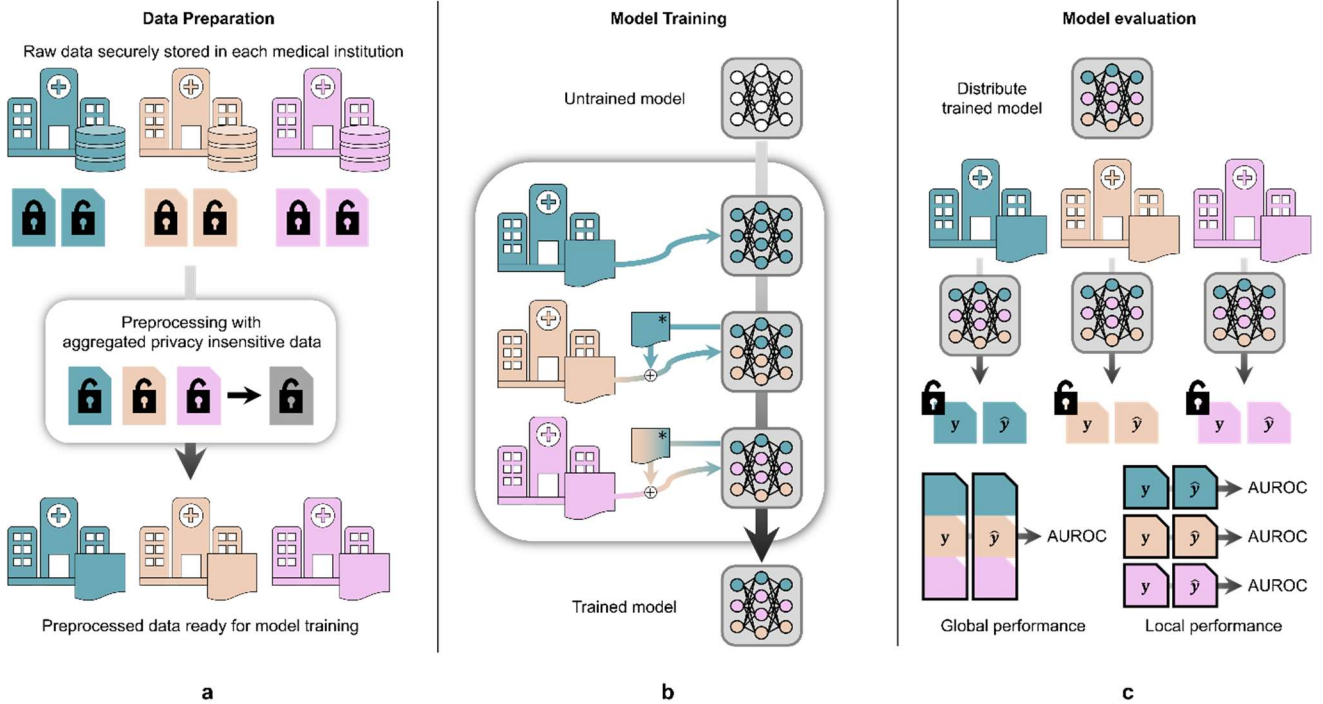


Fig. 1. Overview of privacy-preserving deep learning (PPDL) research pipeline. (a) Data preparation stage. Preprocessing is performed inside each institution using aggregated privacy-insensitive data. Privacy-sensitive data are never shared outside each institution. (b) Model training stage. A neural network model is trained with PPDL training algorithm. The diagram demonstrates review learning (RL). (c) Model evaluation stage. The trained model is distributed to each institution to be evaluated on their test data. Prediction results and target labels can be aggregated to evaluate the model performance since they do not contain privacy-sensitive information. AUROC: area under the receiver operating characteristic curve.

costs. A generative model must be additionally trained for the continual learning of the main deep learning model, which increases computational workload [34, 35]. Furthermore, the generative model must be carried along with the main deep learning model across model transfers, resulting in additional communication burden. Fewer operations and smaller model parameters are beneficial in terms of time, memory, and communication cost. Therefore, such improvements may highly benefit PPDL TL applications.

In this study, we propose “review learning” (RL), a continual learning algorithm based on generative replay that does not require the training of a separate generator. Data samples that represent previously learned information are generated from the synaptic memory of the deep learning model and are used to review knowledge from previous datasets. The continual learning performance of RL was validated via PPDL TL experiments. Its performance was initially verified through simulation PPDL experiments using two types of electronic health record (EHR) data. Next, the performance was further validated through real-world medical multi-institutional PPDL experiments using EHR data stored at Seoul National University Hospital (SNUH), Korea University Medical Center (KUMC), and Ajou Medical Center (AJOUNC). The simulation and the real-world experiments demonstrated that RL allowed the deep learning model to maintain prediction performance on previously trained datasets. The RL algorithm

makes a novel contribution to the continual learning literature by demonstrating that continual learning with generative replay could be performed without a generator, by extracting and reviewing learned knowledge from the synaptic weights of the model.

II. MATERIALS AND METHODS

A. Privacy Preserving Deep Learning Research Pipeline

Catastrophic forgetting and continual learning were evaluated via PPDL TL experiments. The datasets from multiple institutions could not be aggregated owing to data privacy, and the deep learning research pipeline needed modification (Fig. 1). The research process was divided into three stages: data preparation, model training, and model evaluation. During the data preparation stage, the data stored in each institution were preprocessed by sharing the privacy-insensitive statistics of the data. After the data were processed for training, the models were trained using training algorithms, including RL and TL. The trained models were evaluated by copying the models to each institution, where the models predicted test data. The evaluation metrics were measured in global and local scores, which demonstrated the prediction performance on data from all and each institution, respectively. The global score was measured by aggregating privacy-insensitive prediction results for the test data.

> REPLACE THIS LINE WITH YOUR MANUSCRIPT ID NUMBER (DOUBLE-CLICK HERE TO EDIT) <

TABLE I

Summary of cardiovascular disease (CVD) prediction data using EHRs across real medical institutions. Abbreviations: Seoul National University Hospital (SNUH), Korea University Medical Center (KUMC), and Ajou Medical Center (AJOUMC).

Institution name	Control	Case	N	Case ratio
SNUH	38,585	3,381	41,966	8.06%
KUMC	33,878	3,192	37,070	8.61%
AJOUMC	25,067	2,375	27,442	8.65%

B. Simulation Experimental Data

Two types of EHR data were used in the simulation experiment. The first type was a 30-day mortality prediction of sepsis-3 patients [36] from the Medical Information Mart for Intensive Care III database (MIMIC-III) [37]. MIMIC-III is a publicly accessible EHR database from Beth Israel Deaconess Medical Center in Boston, Massachusetts, USA. This database consists of 58,976 admissions and 46,520 unique patients admitted to the intensive care unit between 2001 and 2012. Supplementary data provided by Nianzong et al. [36] were refined for analysis. Rows with invalid age values were removed and feature columns were selected. There were 10 binary columns and 67 continuous columns in total. The refined data can be found from [38].

The second type of EHR data was a cardiovascular disease (CVD) prediction for diabetes patients from SNUH. The study population was extracted from a common data model [39] of SNUH. The task definition was to predict CVD occurrence one year after the patients were diagnosed with diabetes. The initial study population consisted of 52,718 patients who had been diagnosed with type 2 diabetes [40] between 2004 to 2020. However, the patients who were diagnosed with CVD within one year or before diabetes diagnosis were removed since CVD could have been caused by other factors. The patients without any features other than age and sex were also removed. In addition, the patients with CVD were defined as the outcome group, and the rest as the control group. The resulting study population consisted of 40,507 patients, with 3,478 and 37,029 patients in the outcome and control groups, respectively. There were two demographic variables (age, sex), 160 condition variables, 27 measurement variables, and 5 medication variables. The categorical variables were converted into binary columns of each category. There were 167 binary columns and 28 continuous columns in total. In the case of multiple records in continuous columns for the same patient, the last record was used as the representative value. This study was approved by the Institutional Review Board (IRB) of SNUH (No. 2210-042-1366).

C. Heterogeneous Institutional Division for Simulation Experiment

To conduct the simulation PDDL experiment, the data must be allocated to hypothetical institutions. Hypothetical

institutions with feature heterogeneity were generated to simulate the catastrophic forgetting problem. First, the data were divided into control and outcome groups. Second, the Gaussians were generated using a Gaussian mixture model [41] on the continuous columns of each group resulting in total of Gaussians, where n is the number of institutions. Third, the patients from the control and outcome groups were randomly assigned to each institution according to the density of each Gaussian. Fourth, combinations of institutional settings were generated by pairing the number of control and outcome groups. For each setting, local logistic regression models were generated using data from each institution. Fifth, the angles of every pair among the weight vectors of each logistic regression model were measured; the mean angle of the logistic regression model weights demonstrated the data heterogeneity in the current institutional setting. Note that the weight vector was equivalent to the normal vector of the hyperplanes created by the logistic regression model. Finally, the institutional setting with the maximum mean angle between the hyperplanes was selected among the possible settings to maximize feature heterogeneity. Three numbers of hypothetical institutional settings were tested: three, four, and five. The hypothetical institutions were named "local 1," "local 2," ..., and "local n" in descending order of data size. The baseline characteristics in each institutional setting from each simulation data are presented in the Supplementary Materials (Supplementary Fig. 1–6, Supplementary Table 1).

D. Real-World Multi-Institutional Experimental Data

The real-world multi-institutional experiment was performed using the CVD prediction of diabetic patients data from SNUH, KUMC, and AJOUMC. The task definition was identical to that in the simulation experiment, but the variables of the data were modified into common variables across three medical institutions. Patients diagnosed with type 2 diabetes [40] between 2004 to 2020 were included in the data from each institution. The numbers of patients in the outcome and control groups are listed in TABLE I. There were two demographic variables (age, sex), 10 condition variables, 25 measurement variables, and 19 medication variables which were 30 binary columns and 26 continuous columns in total. The baseline characteristics of multi-institutional EHR data are presented in the Supplementary Materials (Supplementary Fig. 7). This study was approved by the IRB of SNUH (2210-042-1366), KUMC (2021AN0236), and AJOUMC (AJIRB-MED-MDB-21-193).

E. Review Learning

RL is a new continual learning algorithm based on generative replay. The algorithm is named after its reviewing process that retains previously learned knowledge by generating samples from the synaptic weights of the model. The RL algorithm is presented here.

RL Algorithm

Input

> REPLACE THIS LINE WITH YOUR MANUSCRIPT ID NUMBER (DOUBLE-CLICK HERE TO EDIT) <

θ_i : Neural network model transferred for the i -th dataset
 $\hat{y}_c^{D'}$: Logits of previous dataset
 D : Current dataset
 N_{review} : Number of samples the model was previously trained on
 N_{real} : Number of samples in D
 // Copy model for knowledge extraction
 $\theta_i^* \leftarrow \theta_i$
 for $epoch$ in max_epoch do
 // Train by jointly optimizing current and generated data
 $D^*, \hat{y}_c^* \leftarrow \text{KnowledgeExtraction}(\theta_i^*, \hat{y}_c^{D'})$
 $\theta_i \leftarrow \text{KnowledgeDistillation}(\theta_i, D, D^*, \hat{y}_c^*)$
 end
 // Store review learning parameters for next transfer
 $\theta_{i+1} \leftarrow \theta_i$
 $\hat{y}_c^D \leftarrow \text{MeasureLogits}(\theta_{i+1}, D, D^*)$
 $N_{review} \leftarrow N_{review} + N_{real}$
 Returns $\theta_{i+1}, \hat{y}_c^D, N_{review}$

RL is composed of two steps: knowledge extraction and knowledge distillation. In the knowledge extraction step, data samples are extracted from the synaptic weights of the model by applying feature visualization [42] to the main classifier model. Data samples are optimized until the logit value of each class equals $\hat{y}_c^{D'}$, which is the logit value of the previous dataset, to generate data samples that are similarly interpreted by the model to the previously trained data. The new logits \hat{y}_c^D are measured after the training on a dataset is complete and before proceeding to the next dataset for further transfers. The number of samples generated is a hyperparameter and does not have to equal the number of samples of the previous dataset because the loss function is weighted-averaged to balance the relative effectiveness of the generated data. The generated data are fed into the main classifier model to calculate the logit value \hat{y}_c^* of each class, which will be used for knowledge distillation [32, 43] in the knowledge distillation step. The knowledge extraction step may be performed once or repeated every epoch. When knowledge extraction is performed more than once, the initial model needs to be copied for multiple knowledge extraction steps.

After the data are generated from the synaptic memory of the model, the model is trained by jointly optimizing the generated data with the current dataset to retain previous knowledge; this constitutes the knowledge distillation step. The loss function in the knowledge distillation step is expressed by (1)–(3). The knowledge distillation [32, 43] loss function, \mathcal{L}_{review} , is computed using the generated data. The \mathcal{L}_{review} uses soft targets for each class, \hat{y}_c^* , and the current model’s logits for generated data, \hat{y}_c . T denotes the temperature of the softmax function [32], which is a hyperparameter. The original loss function, \mathcal{L}_{real} , for the current task is measured using the current dataset. The generated samples and the current dataset are jointly optimized with loss weights, λ_{review} , which represents the relative number of samples. N_{review} refers to the total number of samples on which the model was previously trained, and N_{real} refers to the number of samples in the current

dataset.

$$\mathcal{L}_{review} = -T^2 \sum_{c=1}^{N_{classes}} \hat{y}_c^* \log \hat{y}_c \quad (1)$$

$$\lambda_{review} = \frac{N_{review}}{(N_{real} + N_{review})} \quad (2)$$

$$\mathcal{L} = (1 - \lambda_{review})\mathcal{L}_{real} + \lambda_{review}\mathcal{L}_{review} \quad (3)$$

F. Experimental Setup

1) Simulation Experiment

RL, TL, collaborative data sharing (CDS) [17], and local learning (LL) were evaluated in the simulation experiment. CDS is an upper baseline in performance that could only be tested in a simulation setting, because it trains a model using aggregated dataset and is not privacy-preserving. LL is a lower baseline in performance and refers to training a single model within a local institution. After the hypothetical institutions were generated, data from each institution were divided into training, validation, and test sets with ratios of 0.7, 0.15, and 0.15, respectively. For RL, TL, and LL, the training and validation were performed within each hypothetical institution. For CDS, the local training and validation sets were aggregated to generate merged training and validation sets. A fully connected neural network model with one hidden layer of 32 neurons and a single sigmoid output layer was used. A rectified linear unit (ReLU) followed by a dropout layer with a dropout probability of 50% were applied to the hidden layers. The model parameters were optimized using the Adam [44] optimizer with a learning rate of $1e-3$. The batch size was set to 64 for MIMIC-III data and 256 for CVD prediction data. Binary cross-entropy was used as the loss function, and class weights were applied inverse proportionally to the number of samples for each class to prevent bias in prediction. The number of epochs was 100. Note that in RL, TL, and LL, the model was trained for 100 epochs within each local institution, whereas in CDS, the single server model was trained for 100 epochs. Early stopping was applied by evaluating the area under the receiver operating curve (AUROC) score on the validation set. Validation was performed every 10 updates for MIMIC-III data and 20 steps for CVD prediction data, and the patience was set to 20. Each training algorithm was experimented five times with different model parameter initializations.

The learning rate for the feature visualization in the RL knowledge extraction step was $1e-2$, and 512 samples were generated. The Adam optimizer was used in data generation, and gaussian noise was used as the initial data sample. A sigmoid function was applied to the binary variables as regularization so that the binary variables of the resulting data sample had values between 0 and 1. The temperature T from RL knowledge distillation was set to 5.

2) Real-World Multi-Institutional Experiment

RL, TL, and LL were tested in the real-world multi-institutional experiment. The CDS method was not implemented because privacy-sensitive data could not be aggregated in the real-world experiment. The experiment was conducted by manually visiting each medical institution for the preprocessing, training, and evaluation steps, because the installation of an automated software was restricted owing to their security policies. Privacy-insensitive parameters were

> REPLACE THIS LINE WITH YOUR MANUSCRIPT ID NUMBER (DOUBLE-CLICK HERE TO EDIT) <

TABLE I

Minimum and maximum global scores of PDDL models in the AUROC. RL, TL, and LL stand for review learning, transfer learning, and local learning, respectively. The suffixes “asc” and “desc” in RL and TL indicate the ascending and descending order, respectively, of institutional visits according to the data size. CVD stands for cardiovascular disease.

Simulation setting	Minimum AUROC					Maximum AUROC				
	RL_asc	TL_asc	RL_desc	TL_desc	LL	RL_asc	TL_asc	RL_desc	TL_desc	LL
MIMIC-III, three institutions	0.650	0.612	0.626	0.587	0.578	0.816	0.829	0.792	0.763	0.746
MIMIC-III, four institutions	0.541	0.528	0.675	0.591	0.531	0.773	0.753	0.797	0.783	0.730
MIMIC-III, five institutions	0.656	0.578	0.675	0.543	0.536	0.801	0.794	0.761	0.757	0.736
CVD, three institutions	0.706	0.640	0.713	0.625	0.540	0.863	0.855	0.849	0.849	0.840
CVD, four institutions	0.717	0.648	0.578	0.578	0.563	0.846	0.846	0.837	0.848	0.841
CVD, five institutions	0.711	0.667	0.570	0.570	0.575	0.842	0.833	0.827	0.819	0.828

exported outside each institution after manual inspection by the security officers from each institution. The local statistics of continuous variables, model parameters, and prediction results were shared while keeping the original privacy-sensitive data secure at each institution.

The data from each institution were divided into training, validation, and test sets with ratios of 0.7, 0.15, and 0.15, respectively. A fully connected neural network model with hidden layers of 128, 64, and 32 neurons was used. A ReLU followed by a dropout layer with a dropout probability of 50% were applied to the hidden layers, and a sigmoid function was used in the output layer. The Adam optimizer was used to train the model; the batch size was 128, the learning rate $1e-3$, the weight decay $1e-3$, and the number of epochs 40. Binary cross-entropy was used as the loss function, and class weights were applied in the same way as in the simulation experiment. Early stopping was performed by evaluating the AUROC score on the validation set every 20 updates, and the patience was set to 20. Each training algorithm was experimented three times with different model parameter initializations. The RL hyperparameters were identical to those in the simulation experiment.

G. Preprocessing in Privacy Preserving Deep Learning Setting

Patients from each EHR dataset contained binary, categorical, and continuous variables, and a single feature vector was generated for each patient. Binary variables had a value of 1 if there was a record, and 0 otherwise. Categorical variables were converted into multiple binary columns and encoded in the same way. Continuous variables were standardized using the statistics from the training set. LL models used local statistics to standardize the continuous variables as it assumes no collaboration between institutions, but RL, TL, and CDS used global statistics of training sets from all institutions. Because data could not be aggregated to compute the global statistics, they were derived based on the local statistics using (4)–(6).

$$N = \sum_i^k N_i \quad (4)$$

$$\mu = \frac{\sum_i^k N_i \mu_i}{\sum_i^k N_i} \quad (5)$$

$$\begin{aligned} \sigma &= \frac{\sum_i^k N_i (\mu_i^2 + \sigma_i^2)}{N} - \mu^2 \\ &= \frac{\sum_i^k N_i \left(\mu_i^2 + \left(\frac{1}{N_i} \sum_j^{N_i} x_{i,j}^2 - \mu_i^2 \right) \right)}{N} - \mu^2 \\ &= \frac{\sum_i^k \sum_j^{N_i} x_{i,j}^2}{N} - \mu^2 \\ &= E(X^2) - E(X)^2 \end{aligned} \quad (6)$$

where k is the number of institutions, i the institution number, $x_{i,j}$ the j th data from institution i , μ the mean value, σ the standard deviation, and N the number of samples. Note that μ , σ , and N refer to the global statistics, whereas μ_i , σ_i , and N_i refer to the local statistics from institution i .

H. Evaluation

Two types of metrics were measured. First, the AUROC was computed from the target labels y and model prediction probabilities \hat{y} . Subsequently, the binary model predictions were computed by arbitrarily thresholding the model prediction probabilities at the point where specificity was larger than 0.75. Matthews correlation coefficient (MCC) [45] was measured using the binary model predictions and the target labels. MCC was calculated using (7).

$$MCC = \frac{TP \times TN - FP \times FN}{\sqrt{(TP+FP)(TP+FN)(TN+FP)(TN+FN)}} \quad (7)$$

where TP, TN, FP, and FN stand for true positive, true negative, false positive, and false negative, respectively. Each metric was measured using data from all institutions and data within each institution, which we refer to as global and local score.

Because test data could not be shared outside each institution, the model evaluation was performed in a privacy-preserving manner. As described in Fig. 1(c), a model to be tested was distributed to each institution, and the model made predictions for the test set. Since the target labels y and the predicted probability values \hat{y} did not contain information that could identify each patient, they were not privacy sensitive. Thus, y and \hat{y} for test data were shared to compute the global scores. The local scores were measured using local y and \hat{y} .

> REPLACE THIS LINE WITH YOUR MANUSCRIPT ID NUMBER (DOUBLE-CLICK HERE TO EDIT) <

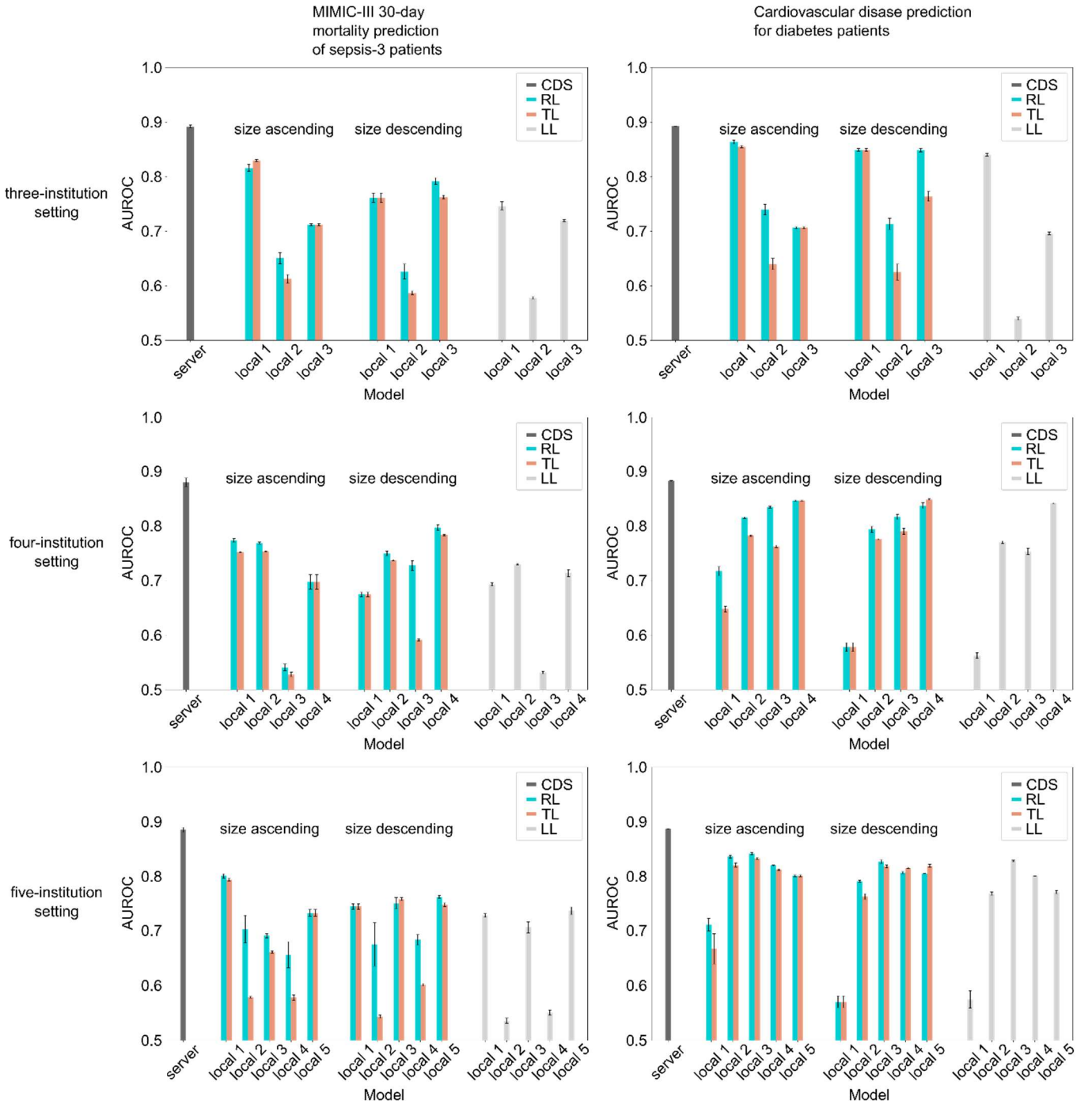


Fig. 2. Global performance scores of simulation experiment measured in AUROC for CDS, RL, TL, and LL. The ascending-size model visits local institutions from local n to local 1, and the descending-size model visits local institutions from local 1 to local n , where n is the number of institutions for a setting. Each experiment was performed five times with different model parameter initializations. The error bars indicate the standard error.

III. RESULTS

A. Inspecting the Review Process in Simulated Multi-Institutional Setting

The simulation study was first performed during the development of RL. Hypothetical institutions with heterogeneous linear features were generated to simulate the

catastrophic forgetting problem under the PDDL setting. An example of heterogeneous data distribution among institutions is presented in Supplementary Fig. 8. RL generated samples from the memory embedded in the synaptic weights of the model and attempted to remember the previously learned knowledge using these samples. To ensure that relevant knowledge was extracted from the model, the generated samples were compared with the original data distribution. An

> REPLACE THIS LINE WITH YOUR MANUSCRIPT ID NUMBER (DOUBLE-CLICK HERE TO EDIT) <

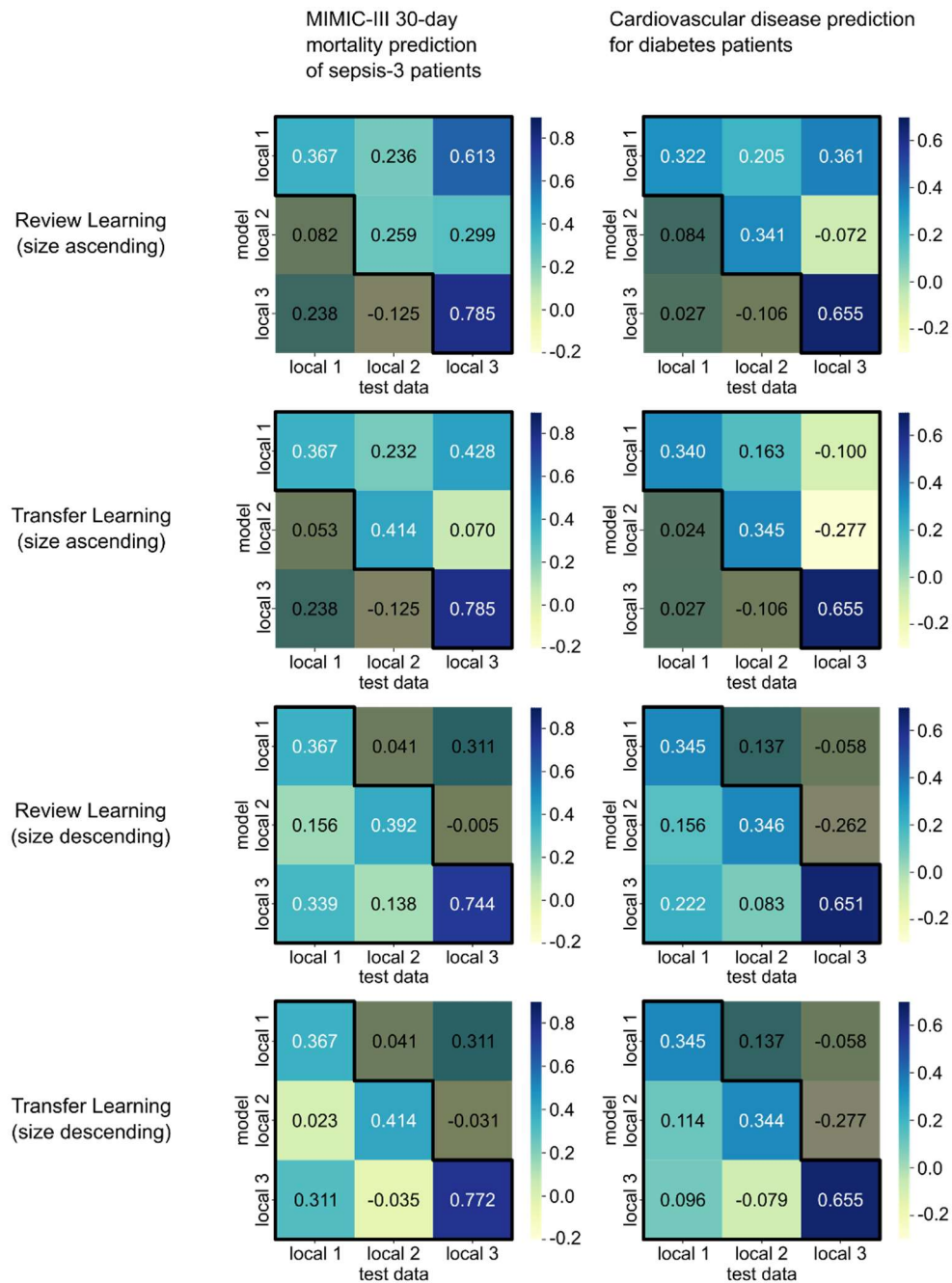


Fig. 3. Local performance scores of simulation experiment for RL and TL. The mean value of Matthews correlation coefficient (MCC) was measured. The three-institutional setting was used to plot the figure. The ascending-size model visits local institutions from local 3 to local 1, and the descending-size model visits local institutions from local 1 to local 3. The performance scores on test data from unvisited institutions are shadowed.

example of data distribution of real and generated data is presented in Supplementary Fig. 9. The real and generated data were placed in similar directions for each of the control and outcome groups, indicating that relevant knowledge could be extracted through the knowledge extraction process of RL.

B. Review Learning Performance in Simulated Multi-Institutional Experiment

RL performance was evaluated through the simulation study of hypothetical institutions before the real-world multi-

institutional study. Global and local performance scores were measured to identify the prediction performance of the model on diverse datasets. The RL, TL, CDS, and LL models were evaluated on two types of binary classification data and three numbers of hypothetical institutions, resulting in six simulation settings. The RL and TL models were trained by visiting the institutions in ascending and descending order of data size, referred to as RL_asc, RL_desc, TL_asc, and TL_desc, respectively.

> REPLACE THIS LINE WITH YOUR MANUSCRIPT ID NUMBER (DOUBLE-CLICK HERE TO EDIT) <

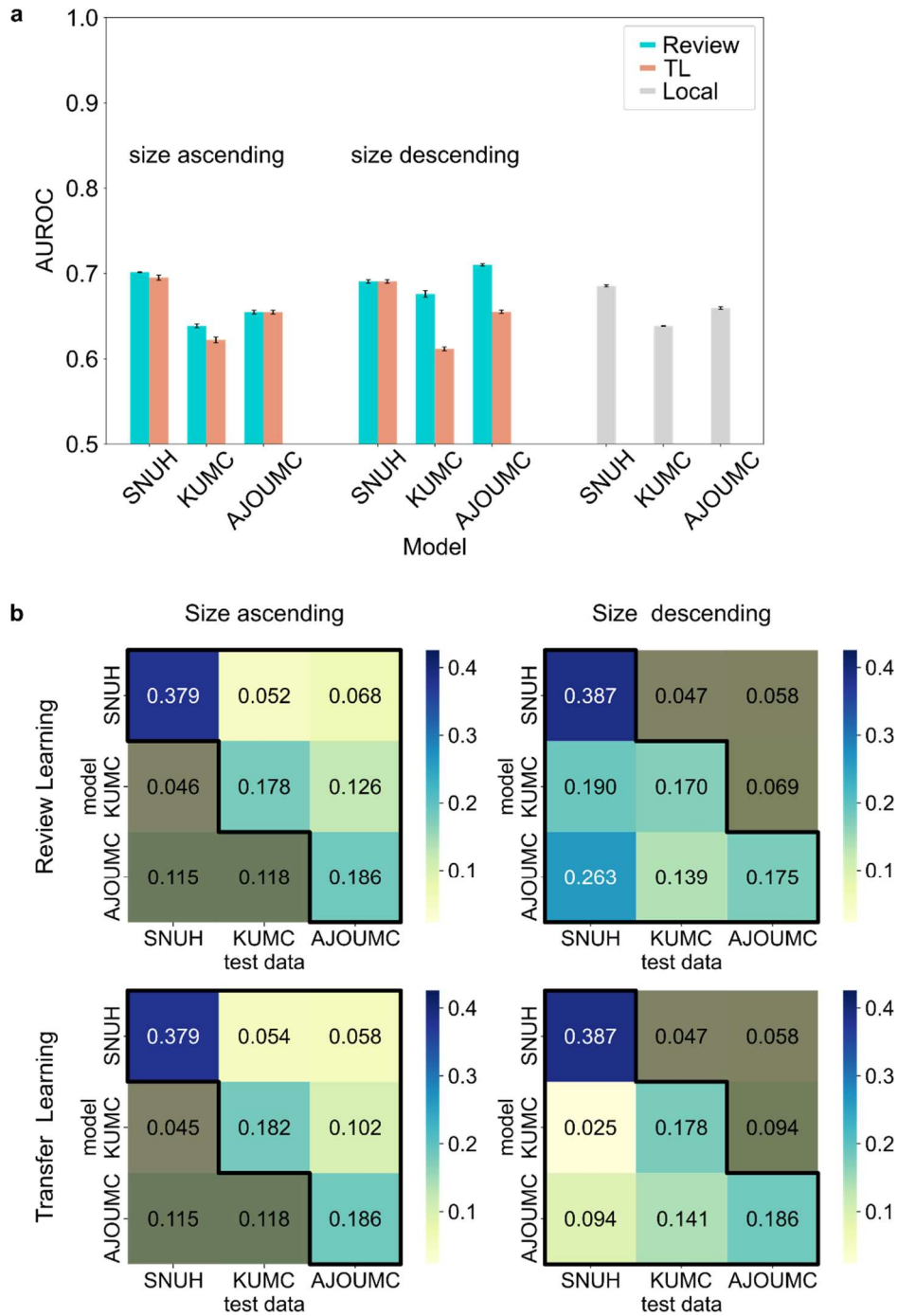


Fig. 4. Performance scores of real-world multi-institutional experiment. (a) Global performance score measured in AUROC. The error bars indicate the standard error. (b) Local performance score. MCC is presented. Abbreviations: Seoul National University Hospital (SNUH), Korea University Medical Center (KUMC), Ajou Medical Center (AJOUMC).

First, the global scores measured in the AUROC are presented in TABLE II and Fig. 2. The TL models suffered from the catastrophic forgetting problem because the global score did not increase steadily but fluctuated significantly as the models were transferred across institutions. However, the RL models suffered less from the catastrophic forgetting problem because the global score fluctuated less as the models were transferred. RL prevented the global score from decreasing substantially when the models visited institutions with

heterogeneous features, e.g. models from local 2 and local 4 in RL_desc and RL_asc, five-institutional setting from the MIMIC-III task (Fig. 2). This can be identified from the minimum global AUROC scores of each simulation experiment, where the minimum scores of RL models were much higher than those of TL models (TABLE II). RL models mostly outperformed TL models in the simulation experiment, but the improvement in the maximum global score across institutions was minimal (TABLE II). Therefore, the continual

> REPLACE THIS LINE WITH YOUR MANUSCRIPT ID NUMBER (DOUBLE-CLICK HERE TO EDIT) <

learning effect of RL prevented the models from forgetting previous knowledge but did not improve the maximum global AUROC score substantially. The global scores of CDS model were the highest in the six settings, which should be expected because the CDS model was trained on aggregated data. LL models were always inferior to RL and TL models except for the five-institutional setting from diabetes dataset, where the performance of LL model was similar to those of RL and TL models. Note that the initial models from RL and TL were identical. Also note that the initial models from RL and TL were different from their corresponding LL models because PPDL models used global statistics in preprocessing whereas LL models used local statistics because no collaboration is assumed between institutions.

The local scores measured in MCC are presented in Fig. 3; for conciseness, only the three-institutional setting is presented. The catastrophic forgetting problem from TL is evident from the local scores since the performance of TL models on test data from previous institutions drops drastically, as shown in the off-diagonal entries in Fig. 3. TL models demonstrated high local scores on recently trained data, which are the diagonal entries in Fig. 3. In contrast, RL models had consistently higher local scores on test data from previous institutions than those of TL models, even when their global scores were similar (e.g., local 1 model from RL_asc from both simulation data). Hence, the knowledge for global and local classification were not identical, and RL models retained the knowledge for local classification whereas TL models lost them. Similar local score patterns were identified in other institutional settings as well, and all scores measured from the simulation experiments are described in Supplementary Fig. 10-11.

C. Review Learning Outperforms Transfer Learning in Real Multi-Institutional Experiment

After the potential of RL was revealed through a simulation study, the RL performance was further verified in a real-world PPDL experiment using data from SNUH, KUMC, and AJOUMC. The data size was in decreasing order from SNUH, KUMC, and AJOUMC (TABLE I). The RL, TL, and LL models were evaluated. The CDS model could not be trained because data could not be aggregated in the real-world experiment.

RL had better performance compared to TL models again in the real-world experiment. The feature distribution of the three medical institutions was heterogeneous, which provoked the catastrophic forgetting problem in the TL models. The forgetting problem can be identified from the fluctuating global score of TL models (Fig. 4(a)) and the low off-diagonal values of TL local scores (Fig. 4(b)). However, all models from RL_asc and RL_desc had a higher global score than their corresponding TL models. The most significant performance improvement was identified from the final model in AJOUMC between RL_desc and TL_desc, where the RL and TL models scored global AUROCs of 0.710 ± 0.002 and 0.655 ± 0.003 , respectively. A local score improvement was apparent in RL_desc, where the performance of the model from the last institution (AJOUMC) on the test set from the first institution

(SNUH) had a local MCC score (0.263 ± 0.013) significantly higher than that of the TL_desc model (0.094 ± 0.014). The off-diagonal entries of RL_desc local scores had higher scores than the TL models (Fig. 4(b)). The RL_asc models had a slightly higher global AUROC than the TL_asc models, but the local scores did not improve drastically. The experimental results are thoroughly described in Supplementary Fig. 12.

IV. DISCUSSION AND CONCLUSION

Catastrophic forgetting prevents the deep learning model from acquiring knowledge sequentially, which restricts the model from learning diverse features across various data. PPDL is one major field of TL application, and catastrophic forgetting damages the model to mispredict test data from previously trained sources. Catastrophic forgetting in PPDL is a major obstacle since the purpose of PPDL is to train a model to learn knowledge from diverse privacy-sensitive data without sharing them. The knowledge within data from diverse sources is likely to be heterogeneous [2, 46], and continual learning needs to be applied to TL to improve performance.

RL, a new continual learning technique based on generative replay, was validated in this study through simulation and real-world PPDL experiments. According to the results, RL outperformed TL in both global and local scores on the test sets from previous institutions, which demonstrates the continual learning effect of RL. Unlike previous works on brain-inspired generative replay, RL did not require a separate generator, which removed the burden of training a generator and the cost of transferring it.

The key to RL is its review process, and the details of reviewing must be thoroughly analyzed so that the model could correctly review previously learned knowledge. One critical aspect of reviewing is the hyperparameters and regularizations. The two steps of the review process, feature visualization [42] and knowledge distillation [43], may vary across data with different modalities, such as image or signals. In the case of generative replay using a generator, the generator learns the relevant data distribution, which includes regularization. However, the data samples extracted from the synaptic memory of the model through feature visualization may be over-optimized because the proper regularizations related to the data are not embedded in the synaptic weights of the main classifier model. Thus, regularizations suitable for certain data modalities, such as random jitter or frequency regularizations, need to be applied to prevent extracting over-optimized samples from the synaptic memory of the model. In PPDL application, this inspection of review process must be completed before transferring to another institution because the generated samples cannot be compared with real data samples, as data from the previous institutions cannot be accessed to preserve privacy.

When generating samples from the synaptic memory of the model, the samples do not have to be realistic as long as the relevant features can be identified. Unlike the objective of generative models, which is to create realistic data, the samples are generated in RL to use them in reviewing knowledge from

> REPLACE THIS LINE WITH YOUR MANUSCRIPT ID NUMBER (DOUBLE-CLICK HERE TO EDIT) <

previous data. Therefore, rather unrealistic generated samples may be sufficient to retain the knowledge of the model. For instance, the binary columns of generated samples in our study contained continuous values between 0 and 1. Although the binary columns of real data only included the values of 0 or 1, the unrealistic generated samples were sufficient to retain the previous knowledge because the deep learning model interpreted all inputs as continuous variables.

RL could be further investigated from several aspects. First, the continual learning performance of RL needs to be compared with other continual learning methods. This study aimed at introducing a new continual learning algorithm and its validation through real-world medical multi-institutional PPDL experiments. The relative performance of RL compared to previous continual learning studies, such as elastic weight consolidation [47], synaptic intelligence [48], and generative replay using a generator [32], remains unknown and needs to be investigated. Another aspect for further research is the usage of different data modalities. RL was validated using EHR data, and the RL performance needs to be tested using data of different modalities. Finally, the performance score of real multi-institutional experimental data needs improvement. Although the real experimental results were sufficient to demonstrate the continual learning performance, the best global score from RL had an AUROC of 0.710 ± 0.002 and an MCC of 0.182 ± 0.002 , which was not significantly large. A higher evaluation score from real experiment could strongly confirm the performance of RL applied in real PPDL settings. With these potential improvements, RL could be a simple but powerful continual learning algorithm that does not require a separate generator.

Jaesung Yoo received the bachelor's degree in electrical engineering along with brain and cognitive sciences from Korea University, South Korea in 2020. He is currently a research assistant at Department of Brain and Cognitive Sciences, Massachusetts Institute of Technology (MIT), Cambridge, MA, USA, and is pursuing M.S. degree from the Department of Electrical Engineering, Korea University, Seoul, South Korea.

He worked as a Research Assistant at Department of Computer Science, Korea University, South Korea; Department of Electrical Engineering, Korea University, South Korea; and Seoul National University Hospital, South Korea. His research interests include computational neuroscience, deep learning, cognitive neuroscience, machine learning, and medical AI.

Sunghyuk Choi: photograph and biography not available at the time of publication.

Ye Seul Yang: photograph and biography not available at the time of publication.

Suhyeon Kim: photograph and biography not available at the time of publication.

Jieun Choi: photograph and biography not available at the time of publication.

Dongkyeong Lim, photograph and biography not available at the time of publication.

Yaeji Lim: photograph and biography not available at the time of publication.

Hyung Joon Joo: photograph and biography not available at the time of publication.

Dae Jung Kim: photograph and biography not available at the time of publication.

Rae Woong Park: photograph and biography not available at the time of publication.

Hyeong-Jin Yoon: photograph and biography not available at the time of publication.

Kwangsoo Kim: photograph and biography not available at the time of publication.

REFERENCES

- [1] Y. LeCun, Y. Bengio, and G. Hinton, "Deep learning," *nature*, vol. 521, no. 7553, pp. 436-444, 2015, doi: <https://doi.org/10.1038/nature14539>.
- [2] E. M. Cahan, T. Hernandez-Boussard, S. Thadaney-Israni, and D. L. Rubin, "Putting the data before the algorithm in big data addressing personalized healthcare," *NPJ digital medicine*, vol. 2, no. 1, pp. 1-6, 2019, doi: <https://doi.org/10.1038/s41746-019-0157-2>.
- [3] Y. Hu, J. Jacob, G. J. Parker, D. J. Hawkes, J. R. Hurst, and D. Stoyanov, "The challenges of deploying artificial intelligence models in a rapidly evolving pandemic," *Nature Machine Intelligence*, vol. 2, no. 6, pp. 298-300, 2020, doi: <https://doi.org/10.1038/s42256-020-0185-2>.
- [4] T. B. Brown *et al.*, "Language models are few-shot learners," *arXiv preprint arXiv:2005.14165*, 2020.
- [5] A. Krizhevsky, I. Sutskever, and G. E. Hinton, "Imagenet classification with deep convolutional neural networks," *Advances in neural information processing systems*, vol. 25, 2012.
- [6] F. Wang, L. P. Casalino, and D. Khullar, "Deep Learning in Medicine—Promise, Progress, and Challenges," *JAMA Internal Medicine*, vol. 179, no. 3, pp. 293-294, 2019, doi: [10.1001/jamainternmed.2018.7117](https://doi.org/10.1001/jamainternmed.2018.7117).
- [7] C. Thapa and S. Camtepe, "Precision health data: Requirements, challenges and existing techniques for data security and privacy," *Computers in Biology and Medicine*, vol. 129, p. 104130, 2021/02/01/ 2021, doi: <https://doi.org/10.1016/j.compbiomed.2020.104130>.
- [8] W. N. Price and I. G. Cohen, "Privacy in the age of medical big data," *Nature Medicine*, vol. 25, no. 1, pp. 37-43, 2019/01/01 2019, doi: [10.1038/s41591-018-0272-7](https://doi.org/10.1038/s41591-018-0272-7).
- [9] K. Weimann and T. O. F. Conrad, "Transfer learning for ECG classification," *Scientific Reports*, vol. 11, no.

> REPLACE THIS LINE WITH YOUR MANUSCRIPT ID NUMBER (DOUBLE-CLICK HERE TO EDIT) <

- 1, p. 5251, 2021/03/04 2021, doi: 10.1038/s41598-021-84374-8.
- [10] Y. Gao and Y. Cui, "Deep transfer learning for reducing health care disparities arising from biomedical data inequality," *Nature Communications*, vol. 11, no. 1, p. 5131, 2020/10/12 2020, doi: 10.1038/s41467-020-18918-3.
- [11] R. Shokri and V. Shmatikov, "Privacy-Preserving Deep Learning," presented at the Proceedings of the 22nd ACM SIGSAC Conference on Computer and Communications Security, Denver, Colorado, USA, 2015. [Online]. Available: <https://doi.org/10.1145/2810103.2813687>.
- [12] K. Chang *et al.*, "Chapter 6 - Privacy-preserving collaborative deep learning methods for multiinstitutional training without sharing patient data," in *Artificial Intelligence in Medicine*, L. Xing, M. L. Giger, and J. K. Min Eds.: Academic Press, 2021, pp. 101-112.
- [13] S. J. Pan and Q. Yang, "A Survey on Transfer Learning," *IEEE Transactions on Knowledge and Data Engineering*, vol. 22, no. 10, pp. 1345-1359, 2010, doi: 10.1109/TKDE.2009.191.
- [14] L. Torrey and J. Shavlik, "Transfer learning," in *Handbook of research on machine learning applications and trends: algorithms, methods, and techniques*: IGI global, 2010, pp. 242-264.
- [15] K. Chang *et al.*, "Distributed deep learning networks among institutions for medical imaging," (in eng), *J Am Med Inform Assoc*, vol. 25, no. 8, pp. 945-954, 2018, doi: 10.1093/jamia/ocy017.
- [16] N. Balachandar, K. Chang, J. Kalpathy-Cramer, and D. L. Rubin, "Accounting for data variability in multi-institutional distributed deep learning for medical imaging," *Journal of the American Medical Informatics Association*, vol. 27, no. 5, pp. 700-708, 2020, doi: 10.1093/jamia/ocaa017.
- [17] M. J. Sheller *et al.*, "Federated learning in medicine: facilitating multi-institutional collaborations without sharing patient data," *Scientific Reports*, vol. 10, no. 1, p. 12598, 2020/07/28 2020, doi: 10.1038/s41598-020-69250-1.
- [18] M. J. Sheller, G. A. Reina, B. Edwards, J. Martin, and S. Bakas, "Multi-institutional deep learning modeling without sharing patient data: A feasibility study on brain tumor segmentation," in *International MICCAI Brainlesion Workshop*, 2018: Springer, pp. 92-104, doi: https://doi.org/10.1007/978-3-030-11723-8_9.
- [19] S. Festag and C. Spreckelsen, "Privacy-Preserving Deep Learning for the Detection of Protected Health Information in Real-World Data: Comparative Evaluation," *JMIR Form Res*, vol. 4, no. 5, p. e14064, 2020/5/5 2020, doi: 10.2196/14064.
- [20] M. Alawad *et al.*, "Privacy-Preserving Deep Learning NLP Models for Cancer Registries," *IEEE Transactions on Emerging Topics in Computing*, no. 01, pp. 1-1, 2020.
- [21] R. M. French, "Catastrophic forgetting in connectionist networks," *Trends in cognitive sciences*, vol. 3, no. 4, pp. 128-135, 1999, doi: [https://doi.org/10.1016/S1364-6613\(99\)01294-2](https://doi.org/10.1016/S1364-6613(99)01294-2).
- [22] M. McCloskey and N. J. Cohen, "Catastrophic Interference in Connectionist Networks: The Sequential Learning Problem," in *Psychology of Learning and Motivation*, vol. 24, G. H. Bower Ed.: Academic Press, 1989, pp. 109-165.
- [23] B. Rasch and J. Born, "Maintaining memories by reactivation," *Current Opinion in Neurobiology*, vol. 17, no. 6, pp. 698-703, 2007/12/01/ 2007, doi: <https://doi.org/10.1016/j.conb.2007.11.007>.
- [24] J. L. McCLELLAND, "Complementary Learning Systems in the Brain: A Connectionist Approach to Explicit and Implicit Cognition and Memory," *Annals of the New York Academy of Sciences*, vol. 843, no. 1, pp. 153-169, 1998, doi: <https://doi.org/10.1111/j.1749-6632.1998.tb08212.x>.
- [25] D. Ji and M. A. Wilson, "Coordinated memory replay in the visual cortex and hippocampus during sleep," *Nature Neuroscience*, vol. 10, no. 1, pp. 100-107, 2007/01/01 2007, doi: 10.1038/nn1825.
- [26] M. F. Carr, S. P. Jadhav, and L. M. Frank, "Hippocampal replay in the awake state: a potential substrate for memory consolidation and retrieval," *Nature Neuroscience*, vol. 14, no. 2, pp. 147-153, 2011/02/01 2011, doi: 10.1038/nn.2732.
- [27] G. I. Parisi, R. Kemker, J. L. Part, C. Kanan, and S. Wermter, "Continual lifelong learning with neural networks: A review," *Neural Networks*, vol. 113, pp. 54-71, 2019/05/01/ 2019, doi: <https://doi.org/10.1016/j.neunet.2019.01.012>.
- [28] D. Lopez-Paz and M. A. Ranzato, "Gradient episodic memory for continual learning," *Advances in neural information processing systems*, vol. 30, 2017.
- [29] D. Rolnick, A. Ahuja, J. Schwarz, T. Lillicrap, and G. Wayne, "Experience replay for continual learning," *Advances in Neural Information Processing Systems*, vol. 32, 2019.
- [30] J. Schwarz *et al.*, "Progress & Compress: A scalable framework for continual learning," presented at the Proceedings of the 35th International Conference on Machine Learning, Proceedings of Machine Learning Research, 2018. [Online]. Available: <https://proceedings.mlr.press/v80/schwarz18a.html>.
- [31] H. Shin, J. K. Lee, J. Kim, and J. Kim, "Continual learning with deep generative replay," *Advances in neural information processing systems*, vol. 30, 2017.
- [32] G. M. van de Ven, H. T. Siegelmann, and A. S. Tolias, "Brain-inspired replay for continual learning with artificial neural networks," *Nature Communications*, vol. 11, no. 1, p. 4069, 2020/08/13 2020, doi: 10.1038/s41467-020-17866-2.
- [33] T. Lesort, H. Caselles-Dupré, M. Garcia-Ortiz, A. Stoian, and D. Filliat, "Generative Models from the perspective of Continual Learning," in *2019 International Joint Conference on Neural Networks (IJCNN)*, 14-19 July 2019 2019, pp. 1-8, doi: 10.1109/IJCNN.2019.8851986.

> REPLACE THIS LINE WITH YOUR MANUSCRIPT ID NUMBER (DOUBLE-CLICK HERE TO EDIT) <

- [34] I. Goodfellow *et al.*, "Generative adversarial nets," *Advances in neural information processing systems*, vol. 27, 2014, 3521-3526, 2017, doi: <https://doi.org/10.1073/pnas.1611835114>.
- [35] A. B. L. Larsen, S. K. Sønderby, H. Larochelle, and O. Winther, "Autoencoding beyond pixels using a learned similarity metric," presented at the Proceedings of The 33rd International Conference on Machine Learning, Proceedings of Machine Learning Research, 2016. [Online]. Available: <https://proceedings.mlr.press/v48/larsen16.html>.
- [36] N. Hou *et al.*, "Predicting 30-days mortality for MIMIC-III patients with sepsis-3: a machine learning approach using XGboost," *Journal of Translational Medicine*, vol. 18, no. 1, p. 462, 2020/12/07 2020, doi: 10.1186/s12967-020-02620-5.
- [37] A. E. W. Johnson *et al.*, "MIMIC-III, a freely accessible critical care database," *Scientific Data*, vol. 3, no. 1, p. 160035, 2016/05/24 2016, doi: 10.1038/sdata.2016.35.
- [38] J. Yoo. *Refined MIMIC-III 30-day mortality prediction of sepsis-3 patients*, doi: 10.21227/qrhd-a469.
- [39] J. M. Overhage, P. B. Ryan, C. G. Reich, A. G. Hartzema, and P. E. Stang, "Validation of a common data model for active safety surveillance research," *Journal of the American Medical Informatics Association*, vol. 19, no. 1, pp. 54-60, 2012.
- [40] A. D. Association, "2. Classification and Diagnosis of Diabetes: Standards of Medical Care in Diabetes—2021," *Diabetes Care*, vol. 44, no. Supplement_1, pp. S15-S33, 2020, doi: 10.2337/dc21-S002.
- [41] D. A. Reynolds, "Gaussian mixture models," *Encyclopedia of biometrics*, vol. 741, no. 659-663, 2009.
- [42] C. Olah, A. Mordvintsev, and L. Schubert, "Feature visualization," *Distill*, vol. 2, no. 11, p. e7, 2017, doi: <https://doi.org/10.23915/distill.00007>.
- [43] G. Hinton, O. Vinyals, and J. Dean, "Distilling the knowledge in a neural network," *arXiv preprint arXiv:1503.02531*, vol. 2, no. 7, 2015, doi: <https://doi.org/10.48550/arXiv.1503.02531>.
- [44] D. P. Kingma and J. Ba, "Adam: A method for stochastic optimization," in *Proceedings of the international conference on learning representations*, San Diego, California, 2015.
- [45] J. Gorodkin, "Comparing two K-category assignments by a K-category correlation coefficient," *Computational Biology and Chemistry*, vol. 28, no. 5, pp. 367-374, 2004/12/01/ 2004, doi: <https://doi.org/10.1016/j.compbiolchem.2004.09.006>.
- [46] S. Shilo, H. Rossman, and E. Segal, "Axes of a revolution: challenges and promises of big data in healthcare," *Nature medicine*, vol. 26, no. 1, pp. 29-38, 2020, doi: <https://doi.org/10.1038/s41591-019-0727-5>.
- [47] J. Kirkpatrick *et al.*, "Overcoming catastrophic forgetting in neural networks," *Proceedings of the national academy of sciences*, vol. 114, no. 13, pp. 3521-3526, 2017, doi: <https://doi.org/10.1073/pnas.1611835114>.
- [48] F. Zenke, B. Poole, and S. Ganguli, "Continual Learning Through Synaptic Intelligence," presented at the Proceedings of the 34th International Conference on Machine Learning, Proceedings of Machine Learning Research, 2017. [Online]. Available: <https://proceedings.mlr.press/v70/zenke17a.html>.